J Nanostruct 15(3): 1324-1332, Summer 2025

RESEARCH PAPER

Study of the Effect of Gamma (γ) Rays on ZnO Thin Films Nanoparticles as a Gas Sensor for NO_2

Mohammed Raheem Abbas [1]*, *Adnan R. Ahmed* [1], *Hassan M. Jaber* [2]

[1] *Department of Physics, College of Education for Pure Sciences, University of Tikrit, Iraq*

[2] *Department of Physics, College of Science, Al–Muthanna University, Iraq*

ARTICLE INFO

Article History:
Received 03 April 2025
Accepted 26 June 2025
Published 01 July 2025

Keywords:
Gamma radiation
Nanoparticles
NO_2 Gas
Structural properties
Zinc oxide thin film

ABSTRACT

In this work, we exposed thin films of zinc oxide ZnO nanoparticles, prepared on glass substrates by using the thermal spray pyrolysis technique, the gamma rays emitted from ^{60}Co with an average energy of 1.25 MeV for different durations to NO_2 detection gas. The XRD analysis revealed a hexagonal wurtzite structure in the thin films, and the increase irradiation time led to an increase in the grain size of the studied ZnO thin films at rates of 15.631, 14.950, and 14.314 nm. ZnO sensors showed highly sensitive responses to NO_2 gas at a concentration of 100 ppm and a temperature of 70 C°. Where the sensitivity before irradiation was equal to (22.81%). Observed that the sensitivity increased by rates of 81.89%, 75.18%, 181.4%, and 242.4% with increased irradiation time. Additionally, radiation exposure reduced the recovery time of the ZnO thin film from 6.039 seconds to 3.111 seconds. Interpreted the improved sensitivity of zinc oxide sensors towards NO_2 gas as a result of radiation-induced changes in surface morphology. These changes led to an increase in surface area and alterations in surface chemistry due to the presence of defects and an abundance of oxygen and zinc vacancies.

How to cite this article
Abbas M., Ahmed A., Jaber H. Study of the Effect of Gamma (γ) Rays on ZnO Thin Films Nanoparticles as a Gas Sensor for NO_2. J Nanostruct, 2025; 15(3):1324-1332. DOI: 10.22052/JNS.2025.03.048

INTRODUCTION

One of the many issues that facing humans in the twenty-first century is the monitoring and detection of dangerous and poisonous gases, such as CO, CH_4, NO_2, etc. Factory and thermal power plants generate nitrogen dioxide (NO_2), a dangerous gas, during combustion. It plays a major role in the atmospheric reactions that produce ozone at ground-level, which is a major component of smog and the main cause of acid rain [1,2]. The environment contains NO_2, a reddish-brown toxic gas with a pungent odor. The American Conference of Governmental Industrial Hygienists has set the threshold value for NO_2 at 3 ppm. Long-term exposure to NO_2 at concentrations higher than 40–100 **µg**/m3 can increase the risk of respiratory disease and may reduce lung function. [3] For the detection of hazardous gases, various metal oxide semiconductor-based sensors (Fe_2O_3 and TiO_2, CuO, WO_3, ZnO) have gained widespread use in recent years. Among these metal oxides, ZnO has gained widespread use as a gas sensing material due to its wide operating temperature range, stability, and flexibility, which make it a promising candidate for sensing applications for hazardous gas detection. Because of its wide energy bandgap (3.37 eV), high binding energy (60 MeV), and excellent mechanical and thermal

* *Corresponding Author Email: gt230078ued@st.tu.edu.iq*

stability at ambient temperature [4][5]. Several post-formation treatments are used to make metal oxide thin films better. These include annealing in a controlled environment and exposing them to high-energy ionizing radiation like gamma rays, protons, and charged particles. Radiation at different doses or fluxes leads to noticeable modifications in the compositional and morphological properties of metal oxides and creates a wide variety of defects [6]. The effect of radiation on metal oxides at high doses leads to two main effects: (1) temporary effects resulting from the generation of electron-hole pairs and (2) permanent effects resulting from the change in the crystal lattice. Therefore, we anticipate that exposing the ZnO sensor to gamma rays could improve its gas sensing capabilities [7]. Researchers Lontio Fomekong, R., & Saruhan, B. studied the gas sensing properties of a thin film of zinc oxide (ZnO) prepared by the (spray-CVD) method and the direction of the gases NO_2, CO, and NO in the temperature range (400-500 ◦C). They demonstrated good selectivity, with the ZnO membrane's selectivity ratio increasing for NO_2 gas compared to CO (1 to 2.4) [8]. Researcher Waikar, Maqsood R., et al, studied the effect of gamma rays on the sensor properties of a thin ZnO membrane prepared chemically, found that after irradiating the membrane with 30 KGy of gamma rays, it became 7.29 times more sensitive to ammonia gas at a 400 ppm concentration, compared to its pre-irradiation value of 1.01[9]. The researcher kumar Anbalagan, Aswin, and his colleagues conducted a study in which they exposed thin films of zinc oxide to varying doses of gamma rays, aiming to create different defects that could impact the sensing of NO_2 gas direction. They demonstrated that the irradiated sensors enhanced their sensitivity by 185%, 160%, and 120% at a 500 ppm concentration under radiation doses of (1.5, 4.5, and 6) KGy. The study confirmed that increasing oxygen vacancies, concentrations of defects, and grain boundaries resulting from radiation can achieve high sensitivity to NO_2 gas [10]. This study aims to increase the sensitivity and effectiveness of sensors that use thin zinc oxide films prepared by the thermal chemical spray method and exposed to different doses of gamma rays to detect NO_2 gas.

MATERIALS AND METHODS

Chemicals like Thomas Baker aqueous zinc nitrate $(NO_3)_2$ $6H_2O$, possessing a molecular weight of 297.5 g/mol and swiftly dissolving in distilled water, were utilized to produce thin zinc oxide films. Determined the solution concentration (0.2 M) by dissolving 2.975 mg of zinc nitrate in 50 ml of distilled water. prepared thin films using the thermal spray pyrolysis approach, which involved spraying the solution onto used glass substrates, which cleans the glass bases well with distilled water, ethanol, and acetone and then with distilled water to remove any stuck-on traces because the presence of impurities greatly affects the accuracy of the resulting measurements. Used a 55 sec spray duration and a 9 sec pause time between depositions to maintain the thermal stability of the glass substrate. After that, repeatedly spray until achieve the desired film thickness. The current investigation determined the ideal spray rate to be 0.35 ml/min, with an air pressure of 1.75 bar,

Fig. 1. shows the appearance of a homemade thermal spray pyrolysis system.

and a nozzle distance of 35 cm from the substrate. We also set the substrate's temperature at (380 ± 5 °C), an important parameter that significantly influences the membrane preparation. Fig. 1 illustrates the appearance of a homemade thermal spray pyrolysis system.

The weighing method was adopted to measure the thickness of thin films after determining the mass of the film deposited on the surface of the substrate with a known area through the following relationship [11].

$$T = \frac{\Delta m}{A \times \rho} \quad (1)$$

Where T the thickness of the thin film is measured in nanometers (nm), A The area of the substrate on which the thin film is deposited, ρ the density of zinc oxide is equal to 5.606 g/cm^3 [12]. Δm Change in mass after deposition. It was determined that the thin film produced for this study had a thickness of (250 ± 10) nm. Exposed the ZnO thin films produced by the thermal spray pyrolysis method to gamma rays using a ^{60}CO source, which produces gamma rays with an energy of 1.25 MeV [13], at different times, the sample before irradiation was indicated as S_0, while the samples exposed to radiation were indicated as (S_{15}, S_{30}, S_{45}, and S_{60}) at times of exposure (15, 30, 45, and 60) minutes, respectively.

Gas sensor measurements

An apparatus that transforms chemical and physical signals into electrical impulses is known as a chemical sensor. This transformation is the result of the difference in the chemical or physical properties of sensitive materials when exposed to detection under the influence of a certain gas [14]. In general, the reducing gas is the electron donor while the oxidizing gas is the electron acceptor. Therefore, the interaction between the metal oxide surface and the gas molecules, which increases or decreases the number of majority carriers, causes the material's resistance or electrical conductivity to change when exposed to gas. So, whether the resistance of the metal oxide goes down or up depends on the type of majority carriers in the semiconductor and the type of gas particles (reduced or oxidized) in the air around it. For p-type materials, gas reduction (donor) increases the resistance of thin films while oxidizing gases (acceptor) decrease it, and vice versa for n-type materials [15,16]. Fig. 2 shows a cross-sectional view of the gas sensor testing system and the homemade test chamber. The unit comprises a cylindrical stainless steel test chamber, hermetically sealed, measuring 27 cm in diameter and 10 cm in height, with a detachable bottom base. The effective volume of the chamber is 5298.5 cm^3; it contains an inlet to allow the flow of the test gas and an air inlet valve to allow atmospheric air after evacuation. The chamber provides a third port for connecting to the vacuum gauge. Through spring-loaded screws, multi-terminal feeding through the chamber base makes it possible to connect the heater assembly and the sensor electrodes to the electrical grid. By opening the valve, we allow the target gas, which is NO_2

Fig. 2. a view of the gas sensor testing system.

with a known concentration, to flow into the test chamber during the test. The variation in the sensor's resistance to the known concentration of the test gas is observed using a digital mustimeter connected to the computer (NI-UT81B).

All samples (S_0, S_{15}, S_{30}, S_{45}, and S_{60}) undergo testing before and after irradiation, with the working temperature set at 70 ◦C and the desired gas concentration set at 100 ppm, NO_2 was produced by reacting copper Cu with concentrated nitric acid HNO_3 to create nitrogen dioxide, which is subsequently converted to nitrogen dioxide upon contact with air [17].

$$4HNO_{3\,(aq)} + Cu_{\,(s)} \rightarrow Cu\,(NO_3)_{2\,(aq)} +$$

$$2NO_{2}\,(g) + 2H_2O_{\,(aq)}$$

Eq. 3 calculates the sensitivity (S) of zinc oxide thin film sensors [18].

$$S = \frac{R_{gas} - R_{air}}{R_{air}} \times 100\% \qquad (3)$$

Where R_{gas} represents the resistance after being exposed to the gas, R_{air} represents the sensor resistance in the air. When the sensor introduces the target gas, it takes the response time to achieve a 90% change in resistance. Similarly, when the sensor stops the target gas, it takes the recovery time to achieve a 90% change in resistance [19].

RESULTS AND DISCUSSIONS

Structural study

Fig. 3 shows an XRD analysis of ZnO thin films before and after exposure to gamma rays. Observed the highest peak intensity at (002), with lower intensity peaks at (100), (101), and (102). XRD analysis confirmed that ZnO has a hexagonal wurtzite crystalline structure [20]. The hexagonal structure of ZnO thin films has the lowest surface energy, which explains why ZnO exhibits a deterministic growth in the (002) level [21] These results are acceptable compared with JCPDS card no. 36-1451 [22]. The average grain size D values of the samples are calculated by Scherrer formula [23].

$$D = \frac{0.94\,\lambda}{\beta \cos\theta} \qquad (4)$$

where θ is Bragg diffraction angle, λ is wavelength of X-rays (0.1540nm) and β is FWHM full width at half the peak's maximum. Considering that the FWHM value depends on the length and width of the peak density, Table 1 reveals that the

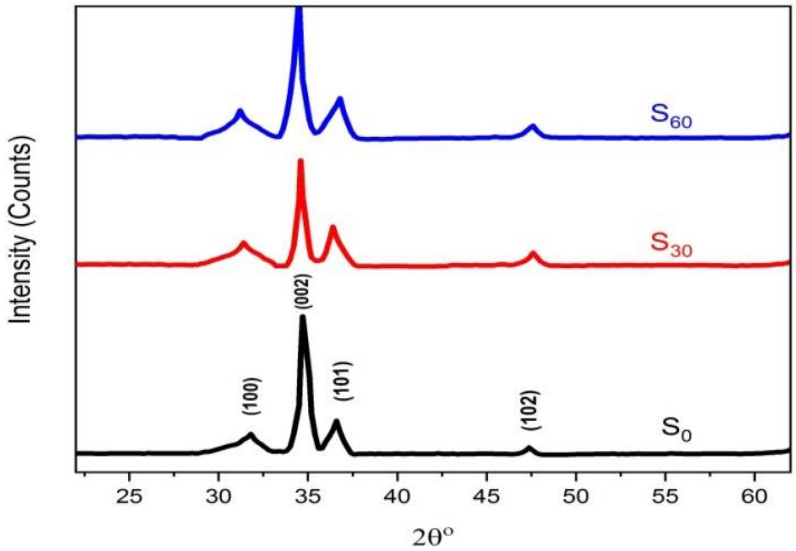

Fig. 3. XRD spectra of ZnO thin films of the samples (S_0, S_{30} and S_{60}).

increase in the irradiation period led to a rise in the FWHM value. Conversely, a decrease in grain size Slightly at a rate of (15.631, 14.950 and 14.314) nm, resulted in an increase in lattice strain Ɛ; its value is calculated through equation (3) [24]. This could suggest the existence of gamma radiation-induced defects, leading to distortions in the crystal lattice [25]. This aligns with the researcher's findings [26].

$$\varepsilon = \frac{\beta \cos\theta}{4} \quad (5)$$

Gas NO_2 Sensing Results

Due to the gas absorption, the resistance of the surface layer of the thin film in the oxidizing gas sensor changes. Examine the sensor properties of all ZnO thin films before and after irradiation as a function of time, at an operating temperature of 70 ◦C. Inject NO_2 gas into a tightly controlled gas chamber with an amount of 100 ppm for varying times, then record the changes in resistance using an electrical measuring device, specifically a digital mustimeter, connected to the computer (NI-UT81B). To find out how sensitive the membranes

Table 1. Analysis of XRD results of ZnO thin films at the highest characteristic peak (002) of the samples (S0, S30 and S60).

Sample	2θ (deg)	hkl	D (nm)	FWHM (deg)	Ɛ*10^{-3}
S_0	34.70	(002)	15.631	0.5325	2.217
S_{30}	34.58	(002)	14.950	0.5567	2.319
S_{60}	34.50	(002)	14.314	0.5813	2.422

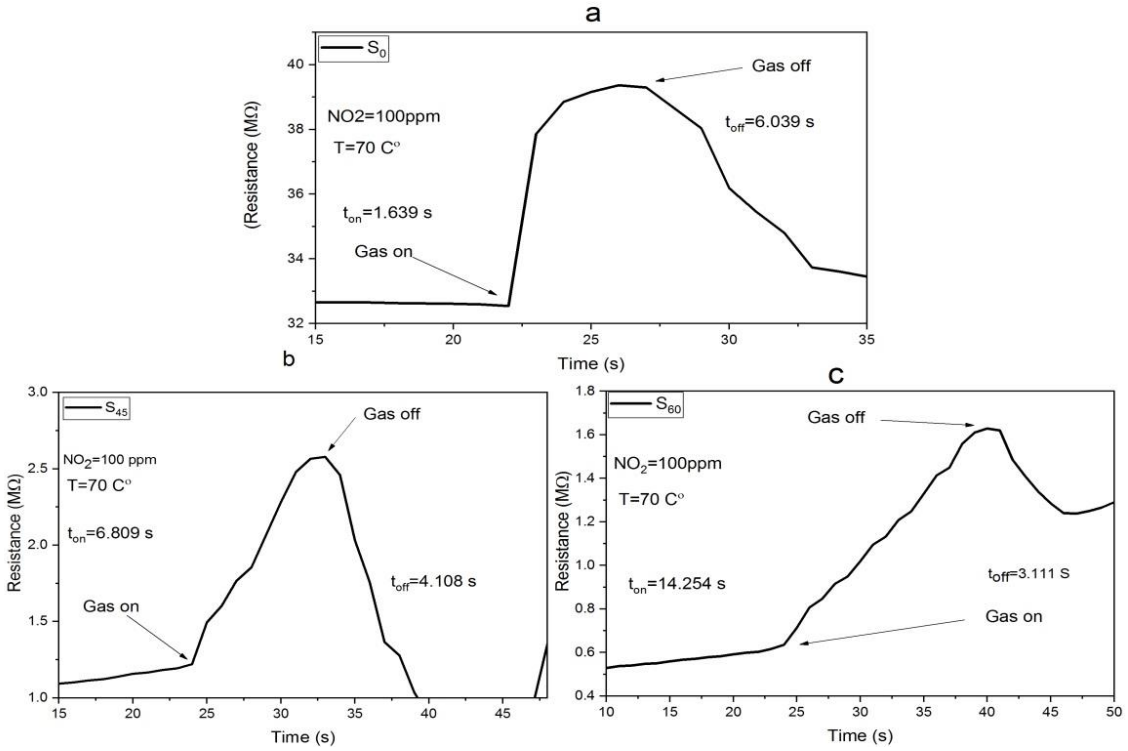

Fig. 4. Illustrates the sensitivity, response time, and recovery time of a ZnO thin film at an operating temperature of 70 C° and a gas amount of 100 ppm for samples (a) S_0, (b) S_{45}, and (c) S_{60}.

were to absorbing the oxidizing gas, a (300±20) nm thick aluminum mask was put on top of the membrane in the shape of a mesh to act as a sensor for the gas that was deposited on the glass. Exposure to the gas NO_2 in the presence of oxygen changes the surface properties of the thin film, altering its resistance, and when the gas stops, it returns to its initial value. Fig. 4 demonstrate an increase in resistance upon exposure of the ZnO thin film to NO_2 gas, an oxidizing gas, both before and after irradiation of the samples (S_0, S_{45}, and S_{60}). The ZnO films contain oxygen voids and zinc voids, as show n-type conductivity [27].

After the zinc oxide-sensitive thin film is exposed to nitrogen dioxide (NO_2), NO_2 is absorbed by the sensitive film, and NO_2 acts as an electron acceptor in the reaction, resulting in increased resistance of the sensor [28]. The surface of the sensor undergoes the following chemical reactions [29]:

$$O_2 + e^-_{ads} \leftrightarrow O^-_{ads} \quad (6)$$

$$NO_{2(ads)} + e^- \rightarrow NO^-_{2(ads)} \quad (7)$$

The above reactions lead to a decrease in the concentration of electrons on the surface of zinc oxide (ZnO), resulting in an increase in the resistance of the material. In addition, the following interaction occurs between O^-_{ads} and $NO_{2(ads)}^-$.

$$NO^-_{2(ads)} + O^-_{ads} \rightarrow 2O^{-2}_{ads} + NO_2 \quad (8)$$

Thus, the periodic interactions continued:

$$NO_{2(g)} + e^- \rightarrow NO^-_{2(ads)} \quad (9)$$

Fig. 5 shows that at a low radiation dose of gamma rays in samples (S_{15}, S_{30}), the excitation process leads to the creation of some charge centers and defects on the surface of the thin film. These generated electrons attract more oxygen, which increases the number of oxygen

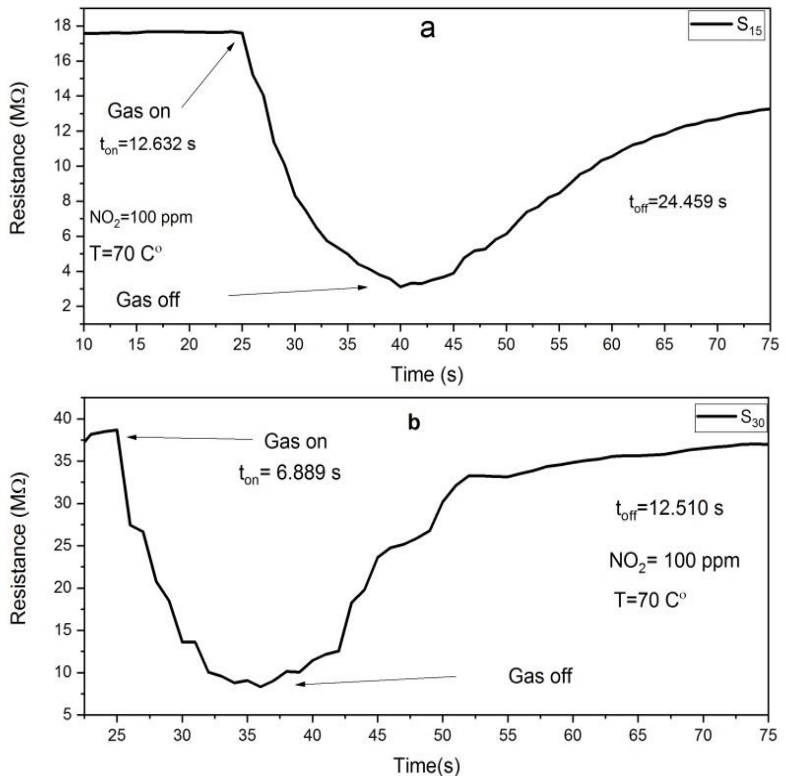

Fig. 5. Illustrates the sensitivity, response time, and recovery time of a ZnO thin film at an operating temperature of 70 C° and a gas amount of 100 ppm for samples (a) S_{15}, (b) S_{30}.

ions absorbed on the surface as the depletion zone decreases further, Additionally, the presence of nitrogen in the surface reactions of the ZnO membrane acts as a shallow surface acceptor, which can contribute to an increase in the concentration of gaps at the surface in ZnO membranes exposed to a low dose, reducing the resistance of the thin films compared to the thin film not exposed to radiation when exposed to the target gas. Defects from deformation (spaced vacancies or atomic overlap) in the ZnO films lead to an increase in the depletion region as the irradiation time for samples (S_{45}, S_{60}) increases. Although the saturation process at this dose reaches the maximum level of absorbed oxygen, the depletion zone does not shrink to the same degree as it did at lower doses. At high doses, the crystal structure deteriorates, which increases the resistance of the film at the surface, as in Fig. 4 above [30,31]. This is consistent with what the researcher indicated [32]. Several reports have shown that testing metal oxide-based gas sensors with nanoparticles alters their surface behavior in terms of resistance [33]. Rani et al. discovered that putting NO_2 gas on SO_2 membranes and then shining a low-dose electron beam on them lowered the surface resistance. When the dose was raised, the resistance went up in the same way it did before irradiation [34]. Majhi et al. also reported that zinc oxide films exposed to gamma rays showed behavior different from the surface resistance at low doses compared to high doses of gamma rays during exposure to NH_3 gas [4].

Sensitivity (S%) was calculated using equation (2), and the response time when opening the gas, changing resistance, and recovery time were also calculated. The above-mentioned figures show different responses depending on the change in radiation dose. Table 2 shows the values of sensitivity, response time, and recovery time calculated before and after irradiation for the ZnO thin film sensor.

The relative change in the response of the sensor after irradiation increased to 242.4% compared to the non-irradiated sensor, which equals 22.81%, as shown in Fig. 6-a. The increase in response when the film is exposed to gamma rays can be attributed to the significant changes in the surface morphology of the ZnO films, as revealed by XRD analysis, which indicated that the grain size decreased with increasing irradiation time, which increases the porosity of the films and leads to an increase in the surface area. This enhances the surface's interaction area with the target gas [35]. In addition, the presence of oxygen and zinc vacancies in the irradiated ZnO films contributes to the increased sensitivity. The presence of interspersed zinc atoms results in a shallow donor level below the conduction band. The electrons at the shallow donor level will acquire sufficient thermal energy to enter the conduction band at operating temperature. Thus, these surface electrons are expected to enhance the oxygen-adsorbing chemical ions on the surface, this results in an enhancement of the sensor's responsiveness [36]. This agrees with the researchers [9,10].

Fig. 6-b, also showed a decrease in the sensor's recovery time (from 6.039 to 3.111 sec) as the irradiation time increased. Recovery time refers to the duration required for the sensor to revert to its initial state (base) following the removal of the target gas. The shorter the recovery time, the better the sensor's performance, as it allows the device to operate faster and respond more frequently to continuous detections, thereby increasing its effectiveness in practical applications such as toxic gas detection [37].

CONCLUSION

This study examined the impact of gamma

Table 2. Shows the calculated values of sensitivity, response time and recovery time for ZnO films for the samples (S0, S15, S30, S45, and S60).

Sample	Sensitivity (S%)	Response time second	Recovery time second
S_0	22.81	1.639	6.039
S_{15}	81.89	12.632	24.459
S_{30}	75.18	6.889	12.510
S_{45}	181.4	6.809	4.108
S_{60}	242.4	14.254	3.111

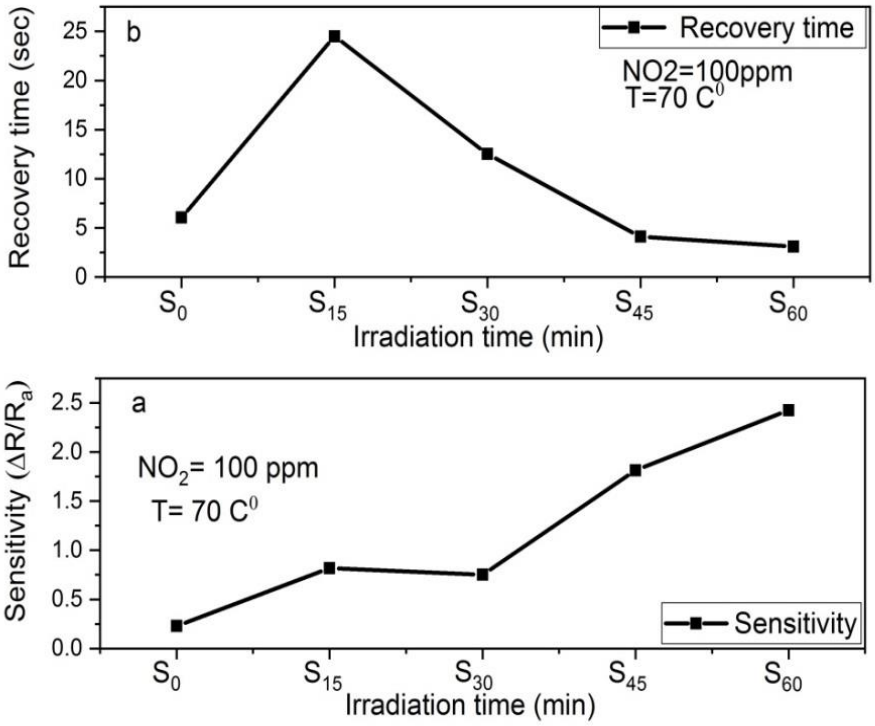

Fig. 6. Shows the values of (a) sensitivity and (b) recovery time, as a function of irradiation time for samples. (S_0, S_{15}, S_{30}, S_{45}, and S_{60}).

radiation on the ZnO thin films under NO_2 gas. For all samples, the XRD test showed the sharpest peak at the (002) level. This level is for the hexagonal wartzite phase of ZnO. In addition, we observed that the grain size decreased at a rate of (15,631, 14,950, and 14,314)nm, with increasing irradiation time. This resulted in a high lattice strain **ε,** which is a sign of defects caused by gamma radiation. Gamma rays greatly affect the relative response of the sensor. As the irradiation time increased, the response increased at a rate of (81.89%, 75.18%, 181.4% and 242.4%) compared to the samples before irradiation, which reached a value of (22.81%). Due to an increase in membrane surface area, the target gas interaction area increased. This was confirmed by XRD analysis. It also showed a decrease in sensor recovery time (from 6.039 to 3.111 sec) with increasing irradiation time. The shorter the recovery time, the better the performance of the sensor, because it allows the device to operate faster and respond more frequently to persistent detections.

CONFLICT OF INTEREST

The authors declare that there is no conflict of interests regarding the publication of this manuscript.

REFERENCES

1. Vanalakar SA, Patil VL, Harale NS, Vhanalakar SA, Gang MG, Kim JY, et al. Controlled growth of ZnO nanorod arrays via wet chemical route for NO2 gas sensor applications. Sensors Actuators B: Chem. 2015;221:1195-1201.
2. Peters JM, Avol E, Gauderman WJ, Linn WS, Navidi W, London SJ, et al. A Study of Twelve Southern California Communities with Differing Levels and Types of Air Pollution. American Journal of Respiratory and Critical Care Medicine. 1999;159(3):768-775.
3. Hamilton RP, Heal MR. Evaluation of method of preparation of passive diffusion tubes for measurement of ambient nitrogen dioxide. J Environ Monit. 2004;6(1):12.
4. Majhi SM, Mirzaei A, Kim HW, Kim SS, Kim TW. Recent advances in energy-saving chemiresistive gas sensors: A review. Nano Energy. 2021;79:105369.
5. Bacaksiz E, Parlak M, Tomakin M, Özçelik A, Karakız M, Altunbaş M. The effects of zinc nitrate, zinc acetate and zinc chloride precursors on investigation of structural and optical properties of ZnO thin films. J Alloys Compd. 2008;466(1-2):447-450.

6. Moon Y-K, Moon D-Y, Lee S, Park J-W. Enhancement of ZnO thin film transistor performance by high-dose proton irradiation. Nuclear Instruments and Methods in Physics Research Section B: Beam Interactions with Materials and Atoms. 2010;268(16):2522-2526.
7. Spieler H. Introduction to radiation-resistant semiconductor devices and circuits. AIP Conference Proceedings: AIP; 1997. p. 23-49.
8. Lontio Fomekong R, Saruhan B. Influence of Humidity on NO_2-Sensing and Selectivity of Spray-CVD Grown ZnO Thin Film above 400 °C. Chemosensors. 2019;7(3):42.
9. Waikar MR, Raste PM, Sonker RK, Gupta V, Tomar M, Shirsat MD, et al. Enhancement in NH_3 sensing performance of ZnO thin-film via gamma-irradiation. J Alloys Compd. 2020;830:154641.
10. Anbalagan Ak, Gupta S, Kumar RR, Tripathy AR, Chaudhary M, Haw S-C, et al. Gamma-ray engineered surface defects on zinc oxide nanorods towards enhanced NO_2 gas sensing performance at room temperature. Sensors Actuators B: Chem. 2022;369:132255.
11. Abdul Majeed EI, Raid AIe, Enad SI, Essam MI. Study the structural and Optical properties of ZnO thin film. Tikrit Journal of Pure Science. 2023;22(1):148-155.
12. Uikey P, Vishwakarma K. Behavior Analysis and Optimization of Zinc Oxide (ZnO) Nanowire using Molecular Dynamic Simulation. International Journal of Engineering Trends and Technology. 2016;38(3):154-157.
13. Reem Saadi K. Influence of gamma radiation on optical constants and optical energy gap of ZnO thin films. Journal of the College of Basic Education. 2023;15(56):105-112.
14. Tri-iodide Reduction Activity of Shape- and Composition-Controlled PtFe Nanostructures as Counter Electrodes in Dye-Sensitized Solar Cells. American Chemical Society (ACS).
15. Deng Y. Sensing Mechanism and Evaluation Criteria of Semiconducting Metal Oxides Gas Sensors. Semiconducting Metal Oxides for Gas Sensing: Springer Singapore; 2019. p. 23-51.
16. Fine GF, Cavanagh LM, Afonja A, Binions R. Metal Oxide Semi-Conductor Gas Sensors in Environmental Monitoring. Sensors. 2010;10(6):5469-5502.
17. Mousavi A. An Investigation of How Nitrogen Monoxide (NO) and Nitrogen Dioxide (NO_2) Are Produced in Oxidations by Nitric Acid (HNO_3). Comments Inorg Chem. 2020;40(6):307-313.
18. Rahmani MB, Keshmiri SH, Shafiei M, Latham K, Wlodarski W, du Plessis J, et al. Transition from n- to p-Type of Spray Pyrolysis Deposited Cu Doped ZnO Thin Films for NO_2 Sensing. Sensor Lett. 2009;7(4):621-628.
19. Chourasia NK, Rawat A, Chourasia RK, Singh H, Kulriya RK, Singh V, et al. Unveiling the potential of $Ti_3C_2T_x$ MXene for gas sensing: recent developments and future perspectives. Materials Advances. 2023;4(23):5948-5973.
20. Ismail A, Alahmad M, Alsabagh M, Abdallah B. Effect of low dose-rate industrial Co-60 gamma irradiation on ZnO thin films: Structural and optical study. Microelectronics Reliability. 2020;104:113556.
21. Malek MF, Mamat MH, Khusaimi Z, Sahdan MZ, Musa MZ, Zainun AR, et al. Sonicated sol–gel preparation of nanoparticulate ZnO thin films with various deposition speeds: The highly preferred c-axis (002) orientation enhances the final properties. J Alloys Compd. 2014;582:12-21.
22. D. S M, Chee FP, Rasmidi R, Alias A, Salleh S, Anuar Mohd Salleh K, et al. Gamma Ray and Neutron Radiation Effects on the Electrical and Structural Properties of n-ZnO/p-$CuGaO_2$ Schottky Diode. ECS Journal of Solid State Science and Technology. 2020;9(4):045019.
23. Abdallah B, Jazmati AK, Kakhia M. Physical, optical and sensing properties of sprayed zinc doped tin oxide films. Optik. 2018;158:1113-1122.
24. I.H.Khudayer IHK, al-Maiyaly BKH, abd al razak AH. Effect of heat treatment on the structural and optical properties of CuIn1-xGaxSe thin films. Paripex - Indian Journal Of Research. 2012;3(5):1-4.
25. Duinong M, Rasmidi R, Chee FP, Moh PY, Salleh S, Mohd Salleh KA, et al. Effect of Gamma Radiation on Structural and Optical Properties of ZnO and Mg-Doped ZnO Films Paired with Monte Carlo Simulation. Coatings. 2022;12(10):1590.
26. Azmy NAN, Abdullah H, Naim NM, Hamid AA, Shaari S, Mokhtar WHMW. Gamma irradiation effect on the structural, morphology and electrical properties of ZnO–CuO doped PVA nanocomposite thin films for Escherichia coli sensor. Radiat Phys Chem. 2014;103:108-113.
27. Nagar S, Gupta SK, Chakrabarti S. Effect of phosphorus irradiation on the structural, electrical, and optical characteristics of ZnO thin films. J Lumin. 2012;132(5):1089-1094.
28. Sharma SL, Maity TK. Effect of gamma radiation on electrical and optical properties of $(TeO_2)_{0.9}$ $(In_2O_3)_{0.1}$ thin films. Bull Mater Sci. 2011;34(1):61-69.
29. Sonker RK, Sabhajeet SR, Singh S, Yadav BC. Synthesis of ZnO nanopetals and its application as NO_2 gas sensor. Mater Lett. 2015;152:189-191.
30. Ranwa S, Barala SS, Fanetti M, Kumar M. Effect of gamma irradiation on Schottky-contacted vertically aligned ZnO nanorod-based hydrogen sensor. Nanotechnology. 2016;27(34):345502.
31. Yun E-J, Jung JW, Han YH, Kim M-W, Lee BC. Effect of high-energy electron beam irradiation on the properties of ZnO thin films prepared by magnetron sputtering. J Appl Phys. 2009;105(12).
32. Baydogan N, Ozdemir O, Cimenoglu H. The improvement in the electrical properties of nanospherical ZnO:Al thin film exposed to irradiation using a Co-60 radioisotope. Radiat Phys Chem. 2013;89:20-27.
33. Prasad AK, Kubinski DJ, Gouma PI. Comparison of sol–gel and ion beam deposited MoO3 thin film gas sensors for selective ammonia detection. Sensors Actuators B: Chem. 2003;93(1-3):25-30.
34. Rani S, Bhatnagar MC, Roy SC, Puri NK, Kanjilal D. p-Type gas-sensing behaviour of undoped SnO2 thin films irradiated with a high-energy ion beam. Sensors Actuators B: Chem. 2008;135(1):35-39.
35. Zeng Y, Lin S, Gu D, Li X. Two-Dimensional Nanomaterials for Gas Sensing Applications: The Role of Theoretical Calculations. Nanomaterials. 2018;8(10):851.
36. Aldosary AF, Shar MA, AlQahtani HR. High-sensitivity detection of ethane and ethylene using gamma-irradiated ZnO chemiresistors. Measurement: Sensors. 2022;24:100600.
37. Huang J, Wan Q. Gas Sensors Based on Semiconducting Metal Oxide One-Dimensional Nanostructures. Sensors. 2009;9(12):9903-9924.